



Scientific Background on the Nobel Prize in Chemistry 2009

STRUCTURE AND FUNCTION OF THE RIBOSOME

Structure and function of the ribosome

This year's Nobel Prize in Chemistry is awarded to **Venkatraman Ramakrishnan, Thomas A. Steitz** and **Ada E. Yonath** for their studies of the structure and function of the ribosome. Their scientific contributions and the historical context are summarized below.

Brief introduction to the ribosome

The ribosome and the central dogma. The genetic information in living systems is stored in the genome sequences of their DNA (deoxyribonucleic acid). A large part of these sequences encode proteins which carry out most of the functional tasks in all extant organisms. The DNA information is made available by *transcription* of the genes to mRNAs (messenger ribonucleic acids) that subsequently are *translated* into the various amino acid sequences of all the proteins of an organism. This is the central dogma (Crick, 1970) of molecular biology in its simplest form (Figure 1)

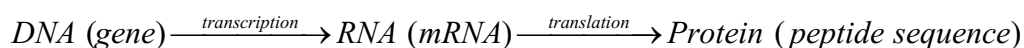


Figure 1. The central dogma revisited.

The genetic information in DNA is preserved by *replication* of the genome (Watson and Crick, 1953a, b) carried out by DNA polymerase (Kornberg, 1969) so that each daughter cell can receive one genome copy at every cell division. In all organisms, transcription of DNA into mRNA is carried out by RNA polymerase (Kornberg, 2007), and translation of mRNA is carried out by the ribosome. Each mRNA sequence consists of ribonucleotides with either one of four bases: A (adenine), C (cytosine), G (guanine) and U (uracil). Each amino acid is encoded by one or several triplets of bases (codons), *e.g.* UUU or UUC for the amino acid phenylalanine, termination of translation by the triplets UAG, UAA or UGA and initiation of translation mainly by AUG, also encoding the amino acid methionine (Nirenberg et al., 1965; Soll et al., 1965). The mRNA sequence is decoded starting from an AUG codon, followed by a sequence of codons, specifying the order of insertion of amino acids in the nascent protein, which is followed by a termination codon, signaling that the protein is ready for dissociation from the ribosome for subsequent folding into its functional state. The link between the messenger RNA and the peptide sequence is transfer RNA (tRNA), in line with the adaptor hypothesis (Crick, 1958). In the bacterial cell there are about 50 different types of tRNA molecules, each composed of about 75 nucleotides. They have a CCA-end, to which an amino acid can be linked by an ester bond, and an anticodon, which can read an mRNA codon cognate to the amino acid linked to the CCA-end of the tRNA. For each amino acid there is an enzyme recognizing tRNAs with an anticodon complementary to the mRNA codon cognate to this amino acid. Accordingly, the enzyme recognizes the amino acid *and* its cognate tRNA(s) and couples them together at the expense of ATP hydrolysis to a high standard free energy complex called aminoacyl-tRNA.



Components of the ribosome. The bacterial (70S) ribosome consists of a small (30S) and a large (50S) subunit, with molecular weights of about 800 000 and 1 500 000 Dalton (Da), respectively, where S stands for the Svedberg unit for sedimentation velocity. The 30S subunit consists of about 20 different proteins and a sequence, 16S, of ribosomal RNA (rRNA) containing about 1600 nucleotides. The 50S subunit consists of about 33 different proteins, a 23S rRNA sequence with about 2900 nucleotides, and a 5S rRNA sequence with about 120 nucleotides. Ribosomes from eukaryotes are larger and more complex than those from prokaryotes, but from everything we know ribosomes from all three kingdoms of life function according to the very same principles. The ribosome has three binding sites for tRNA, the A (aminoacyl) site, the P (peptidyl) site and the E (exit) site, formed in the inter subunit interface (Figures 2, 3). The mRNA binds in a track around the neck of the 30S subunit, through which it can move in a stepwise manner, one codon at the time, during peptide elongation of a nascent chain, as described below.

Initiation of protein synthesis. In bacteria, the synthesis of a protein, according to the instruction of its mRNA sequence, starts when the mRNA binds to the ribosomal 30S subunit, where its so called Shine and Dalgarno (SD) leader sequence contacts the anti-SD sequence of 16S rRNA. This event is followed by binding of the initiator tRNA, charged with formylated methionine, to the P site in a reaction step greatly accelerated by the three initiation factors 1 (IF1), 2 (IF2, a GTPase) and 3 (IF3). When mRNA and initiator tRNA are in place, the 50S subunit docks to the pre-initiation 30S complex in an initiation factor aided reaction and the ribosomal 70S ribosome is formed (Antoun et al., 2006), with the mRNA in the correct reading frame, initiator tRNA in the P site and the empty A site programmed with the first internal codon of the protein to be synthesized. The ribosome has now left the initiation phase and entered the peptide elongation phase.

Peptide elongation and translocation. In the elongation phase (Figure 2), aminoacyl-tRNAs enter the A site in complex with the protein elongation factor Tu (EF-Tu, a GTPase). In response to cognate codon-anticodon interaction, GTP is rapidly hydrolyzed on EF-Tu allowing for aminoacyl-tRNA accommodation in the A site, followed by peptide bond formation catalyzed in the peptidyl-transfer center (PTC) of the 50S subunit (Rodnina et al., 2007). The ribosome now has a peptidyl-tRNA in the A site, with tRNA and nascent peptide chain elongated by one amino acid and a deacylated tRNA in the P site; it is in the pre-translocation state.

In the next major elongation step, elongation factor G (EF-G, a GTPase) binds to the A-site bound peptidyl-tRNA and induces its *translocation* from A to P site and translocation of the A-site bound tRNA to E site, concomitant with a forward move of the mRNA in its reading frame, so that the A site becomes programmed with the next codon to be read by an aminoacyl-tRNA (Frank et al., 2007). Peptide elongation is repeated, until a stop codon appears in the A site.

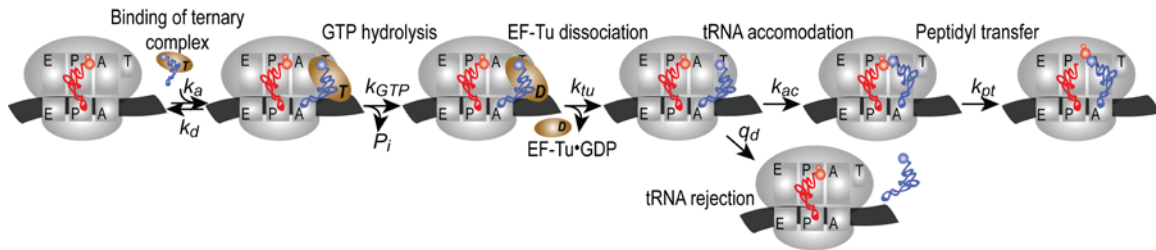


Figure 2. Scheme for ribosomal decoding and peptidyl-transfer. Ternary complex binds to the ribosomal A site with rate constant k_a and dissociates with rate constant k_d . GTP on EF-Tu is hydrolyzed with rate constant k_{GTP} , EF-Tu leaves with rate constant k_{tu} , tRNA accommodates in the A site with rate constant k_{ac} or dissociates by proofreading with rate constant q_d and peptidyl-transfer occurs with rate constant k_{pt} . The tRNAs are drawn to show their familiar L-shape, rather than their exact orientation on the ribosome.

Cryo-electron microscopy (cryo-EM) views of the ribosome bound to ternary complex and the ribosome with peptidyl-tRNA in the A site and deacylated tRNAs in the P and E sites are shown in Figure 3 (Valle et al., 2003).

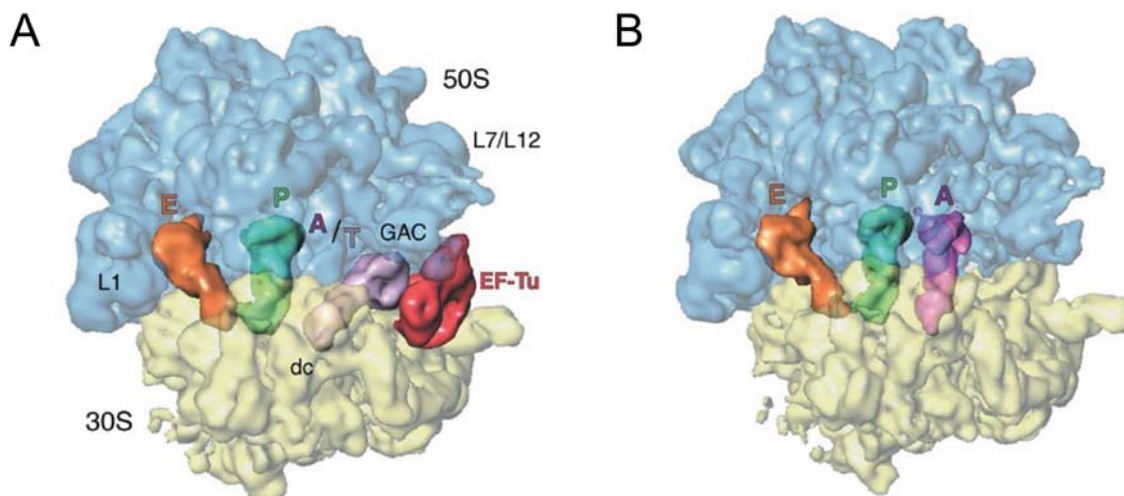


Figure 3. Binding of EF-Tu and tRNAs to the ribosome seen by cryo-EM. (A) Aminoacyl-tRNA in A/T site in ternary complex, peptidyl-tRNA in P site and deacylated tRNA in E site. (B) Pre-translocation ribosome with peptidyl-tRNA in A site, deacylated tRNAs in P and E site (From Valle et al., 2003).

Termination of protein synthesis and ribosomal recycling. Stop codons are read exclusively by class-1 release factors 1 (RF1, codons UAA, UAG) and 2 (RF2, codons UAA, UGA). They induce hydrolysis of the ester bond linking a finished protein chain with the P-site bound tRNA, leading to rapid release and subsequent folding of the protein into its functional form (Kisselev and Buckingham, 2000) and rapid dissociation of the class-1 release factors by the class-2 release factor 3 (RF3, a GTPase) (Zavialov et al., 2002). Subsequently, the ribosome is recycled to a new round of initiation with a new mRNA by the joint action of ribosomal recycling factor (RRF) and EF-G (Karimi et al., 1999).

Long standing mysteries in ribosome function. From this brief account of ribosome function it follows that the ribosome catalyzes two chemical reaction steps involving covalent bonds: peptide bond formation and ester bond hydrolysis during termination. It also follows that there exist delicate accuracy problems during protein elongation and termination. That is, in elongation phase an aminoacyl-tRNA cognate to an amino acid-encoding A-site codon (sense codon) must be efficiently selected and, at the same time, all near-cognate aminoacyl-tRNAs or class-1 release factors must be rejected with very high probability of avoiding amino acid substitution or premature termination errors. The first type of errors would lead to reduced or altered activity of synthesized proteins and the second to greatly reduced ability of the ribosome to produce ready made proteins, i.e. to a large reduction of the ribosome's processivity. Furthermore, a class-1 release factor must be efficiently selected when there is a stop codon (nonsense codon) in the A site, while read-through of a stop codon by an aminocyl-tRNA must be avoided.

The chemical mechanisms of the covalent reaction steps carried out by the ribosome remained mysterious during decades of intense work on the bacterial ribosome by a large number of groups. How tRNAs and class-1 release factors manage to discriminate so precisely between their cognate and near-cognate codons in a ribosome dependent manner were other unanswered questions. Finally, how antibiotic drugs and ribosomal mutations can tune the accuracy of codon reading up or down have also remained obscure. The clarification of these and other central questions concerning normal ribosome function and how ribosome function is perturbed by the action of antibiotic drugs or mutations depended on the advent of crystal structures at high resolution of ribosomal subunits, the whole ribosome and important functional complexes of the ribosome, its subunits and, finally, of the 70S ribosome itself.

The path to high resolution crystal structures of ribosomal subunits

The early stage of ribosome crystallography. The ribosome, with its molecular weight of about 2.5 MDa is not only large but, unlike many virus particles, does not display symmetry properties that would facilitate crystallization and structure determination. In the years around 1980 it was therefore unclear whether crystals of the ribosome diffracting to high resolution ($\sim 3\text{\AA}$ or less) could ever be found and, granted the existence of such crystals, whether the phase problem could be overcome and structures obtained. In this context, the report on three-dimensional crystals of the ribosomal 50S subunit from the thermophile bacterium *Geobacillus (G.) stearothermophilus* (previously called *Bacillus stearothermophilus*) in 1980 by Ada Yonath and colleagues (Yonath et al., 1980) was therefore a significant step forward. The first crystal structures of the 50S subunit to give crystallographic information were subsequently obtained by Yonath for *G. stearothermophilus* (Yonath et al., 1984) and the archaeon *Haloarcola (H.) marismortui* (Shevack et al., 1985) followed by crystals from the same organism diffracting to 6\AA (Makowski et al., 1987). Crystals of the 70S ribosome and its isolated 30S subunit for *Thermus (T.) thermophilus* were reported by (Trakhanov et al., 1987) and for the 30S subunit from the same organism by Yonath and collaborators (Glötz et al., 1987). These early crystals diffracted to about 10\AA , and could in principle never lead to structures at a resolution that would allow the construction of a detailed atomic model. The

finding some years later that carefully prepared crystals from the 50S subunit from *H. marismortui* could diffract to 3Å (von Bohlen et al., 1991) was therefore another important step forward towards ribosome structures at high resolution taken by Yonath and collaborators. The ultimate success in this quest would partially depend on improved quality of ribosomal crystals by, e.g., application of cryo-crystallography (Garman, 1999) to minimize radiation damage of ribosomal crystals, as pioneered by Yonath, Hope and collaborators (Hope et al., 1989). There were also other technical improvements that made ribosome crystallography feasible. Among these were the introduction of CCD area-detectors for precise and automated analysis of x-ray diffraction patterns and tunable synchrotron radiation sources for optimal use of anomalous scattering for phase determination (Hendrickson et al., 1997; Holmes and Rosenbaum, 1998; Phillips et al., 1977).

In summary, Ada Yonath's work throughout the 1980s has been instrumental for obtaining the robust and well diffracting ribosome crystals that eventually led to high resolution structures of the two ribosomal subunits. This would take another ten years, however, with new main players, including Thomas Steitz with collaborators from Yale University, USA and Venkatraman Ramakrishnan with collaborators from MRC, Cambridge, UK.

The ribosome and its subunits at high resolution. Ada Yonath had made significant contributions to obtain a high resolution structure of the 50S ribosomal subunit by her crystals from *H. marismortui* diffracting beyond 3Å resolution (Shevack et al., 1985; von Bohlen et al., 1991; Yonath et al., 1980). However, Steitz and collaborators were the first to solve the profoundly challenging phase problem of the 50S structure from *H. marismortui*. Since the phase problem had not been solved for the 30S subunit at this time, this meant a decisive breakthrough in ribosomal crystallography. For this, they initially used a cryo-electron microscopy (cryo-EM) reconstruction of the ribosomal 50S subunit from J. Frank (Frank et al., 1995), along with multiple isomorphous replacement and anomalous scattering techniques. This led them to a low resolution structure of the 50S structure (Ban et al., 1998). This reconstruction at 9Å resolution (Figure 4) displayed right-handed double helical density typical of A-form RNA. It demonstrated for the first time that the phase problem was tractable for ribosomal subunits and even the whole 70S ribosome. This strongly suggested that both high resolution structures of ribosomal subunits and the whole ribosome were within near reach. One year later, a middle (5Å) resolution structure of the 50S subunit (*H. marismortui*) was reported by Steitz and collaborators (Figure 4) (Ban et al., 1999). The same year a 5.5 Å resolution structure of the 30S subunit (*T. thermophilus*) appeared from Ramakrishnan and collaborators (Clemons et al., 1999) soon followed by a 4.5 Å resolution structure of the *T. thermophilus* 30S subunit from Yonath and collaborators (Tocij et al., 1999). In the same year, Noller and collaborators reported the structure of the 70S ribosome from *T. thermophilus* at 7.8Å resolution, containing tRNAs in the ribosomal A, P and E sites and an mRNA in the track around the neck of the 30S subunit (Cate et al., 1999). Neither one of these structures displayed high enough resolution to construct complete atomic models, but they provided the necessary stepping stones on the path to the high resolution structures to rapidly follow.

In the year 2000 Steitz and collaborators reported the 50S structure from *H. marismortui* at 2.4Å resolution (Figure 4) (Ban et al., 2000; Nissen et al., 2000), while

Ramakrishnan reported the 30S structure from *T. thermophilus* at 3.0Å (Wimberly et al., 2000) and Yonath the structure from the same subunit at 3.3Å (Schlutzen et al., 2000) resolution. The two 30S structures displayed very similar overall structures, with some differences at the atomic level. These discrepancies were removed by a subsequent structure reported from Yonath's laboratory at 3.2Å resolution (Pioletti et al., 2001). The path from low (Ban et al., 1998) via intermediate (Ban et al., 1999) to high (Ban et al., 2000) resolution 50S subunit structures is illustrated in Figure 4. In 2001, Yonath and collaborators obtained a high resolution structure of the 50S subunit from the Gram positive bacterium *Deinococcus (D.) radiodurans* (Harms et al., 2001), particularly suitable for studies of antibiotics targeting the bacterial ribosome (see Section 6 below).

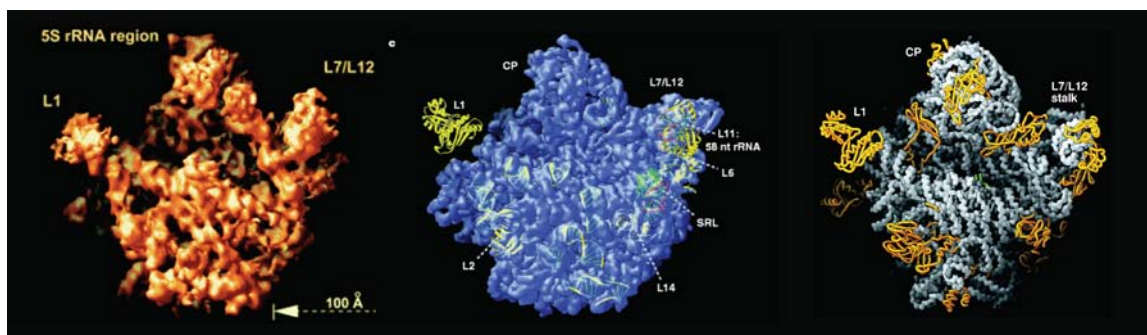


Figure 4. The path to the 50S subunit structure at high resolution. The 50S subunit structure at 9Å resolution (left, 1998), 5Å resolution (middle, 1999) and 2.4Å resolution (right, 2000) (From Ban et al., 1998; 1999; 2000).

In 2001, Noller and collaborators reported the crystal structure of the 70S ribosome from *T. thermophilus* at 5.5Å resolution (Yusupov et al., 2001), but a structure of the whole 70S particle at high resolution (3.5Å) was first obtained by Cate and collaborators for an empty ribosome from *Escherichia (E.) coli* (Schuwirth et al., 2005).

When the structures of the two ribosomal subunits had been obtained at high resolution, it was clear that a radical change in the boundary conditions of ribosome research had occurred. One finding that initially caught considerable attention was that the peptidyl-transferase centre, where peptide bond formation is catalyzed (Figure 2), seemed to lack ribosomal protein components. In fact, there was no visible peptide chain within 18Å from the identified peptidyl-transferase centre (Nissen et al., 2000), which by many was taken as the ultimate proof of previous suggestions, *e.g.* (Noller et al., 1992), that the ribosome is a ribozyme, *i.e.* an enzyme deriving its catalytic power from RNA and not protein. This result had been anticipated, not the least by the support it gave to the view that the present biochemical world, in which proteins carry out the vast majority of biochemical functions, has been preceded by an “RNA world”, where RNA was not only an information carrier, but also performed the functional tasks (See, however, below section 6).

The structures of the two ribosomal subunits rapidly provided a wealth of new insights in the structural folds of RNA and the binding properties of antibiotics (See below, section 5).

However, the answers to fundamental questions concerning the accuracy of tRNA selection during protein elongation (See below, section 3) and the mechanism of peptidyl-transfer (See below, section 4) required more crystallographic work in combination with biochemistry and computational approaches.

Ribosome structure and the accuracy of mRNA translation

Accurate translation of the genetic code to sequences of amino acids by recognition of aminoacyl-tRNAs cognate to mRNA codons displayed in the A site ultimately depends on the standard free energy difference ($\Delta\Delta G^\circ$) between cognate and non-cognate codon-anticodon pairs. Given these $\Delta\Delta G^\circ$ -values for the competition between cognate and non-cognate tRNAs at all the 61 amino acid encoding (sense) codons in mRNAs, the ribosome can enhance the accuracy and thereby reduce the frequency of amino acid substitution errors in nascent peptide chains by the principle of proofreading (Hopfield, 1974; Ninio, 1975). Aminoacyl-tRNAs enter the ribosome in ternary complexes with EF-Tu and GTP. Among these the cognate ternary complexes are selected for GTP hydrolysis with high probability, while non-cognate ternary complexes dissociate with high probability (Figure 2). After GTP hydrolysis, cognate aminoacyl-tRNAs are accommodated in the ribosomal A site as acceptors in the peptidyl-transfer reaction with high probability, while non-cognate aminoacyl-tRNAs are rejected with high probability in the proofreading step (Gromadski and Rodnina, 2004; Pape et al., 1999; Ruusala et al., 1982; Thompson and Stone, 1977). In this way, the same standard free energy difference between cognate and non-cognate tRNAs can be used twice ($n=2$) or several times ($n>2$) (Ehrenberg and Blomberg, 1980; Freter and Savageau, 1980), so that the upper limit, d , of the current accuracy, $A < d$, can be increased from $A < d = e^{\Delta\Delta G^\circ/RT}$ to $A < d^n = e^{n\Delta\Delta G^\circ/RT}$. Here, A is defined as the ratio between cognate and non-cognate peptide bonds at equal concentrations of cognate and non-cognate ternary complexes. The ribosome could also, in principle, amplify the accuracy A is by increasing the standard free energy difference $\Delta\Delta G^\circ$ itself, but how this could be achieved had been a long-lasting riddle in ribosome research.

The genetic code is redundant; there are twenty canonical amino acids but 61 sense codons, all of which are used in mRNAs. One solution to this problem is provided by the existence of several iso-accepting tRNAs for the same amino acid. In *E. coli* there are for example five iso-accepting tRNAs for the amino acid leucine. Another solution is that one and the same tRNA can read several codons by accepting mismatches in the third codon position according to the wobble hypothesis (Crick, 1966). In *E. coli*, to exemplify, tRNA^{Phe} (anticodon GAA) reads the two phenylalanine codons UUU, UUC, the isoacceptor tRNA^{Leu2} (anticodon GAG) reads the leucine codons CUU, CUC and tRNA^{Leu3} (anticodon UAG) reads CUG, CUA and CUU. The physical chemical basis for the generally occurring third codon position wobble has been another unanswered question during more than forty years of ribosome research.

The accuracy of codon reading on the ribosome can be tuned up or down by mutations in ribosomal RNA and ribosomal proteins, and some ribosome targeting antibiotics have profound effects on the accuracy of codon reading. These accuracy tuning features have also remained mysterious, since they often relate to events far from the decoding centre (See dc in Figure 3) of the 30S ribosomal subunit, where the codon-anticodon interactions take place

(Ogle and Ramakrishnan, 2005). Based on 30S subunit structures at high resolution in complexes with various ligands, the questions (i) how the ribosome can enhance the $\Delta\Delta G^\circ$ - values for tRNA discrimination in initial selection *and* proofreading, (ii) how the wobble mechanism works and (iii) how ribosomal mutations and antibiotics affect ribosomal accuracy have been answered in a simple and coherent manner by Ramakrishnan and collaborators.

In line with previous NMR experiments (Fourmy et al., 1998; Yoshizawa et al., 1999) it was found (Carter et al., 2000) that the presence of the translation error enhancing aminoglycoside drug paromomycin in the *T. thermophilus* crystal structure of the 30S subunit induced bases 1492 and 1493 to “flip out” and be placed in putative contact with the minor groove of the codon-anticodon helix. It was suggested that these bases may allow for recognition, not only of the H-bond energies due to Watson-Crick base pairing, but also of the *geometry* of that part of the codon- anticodon helix that involves the first two codon bases, while the wobble base pair would be monitored less stringently by such a $\Delta\Delta G^\circ$ -enhancing mechanism (Figure 5).

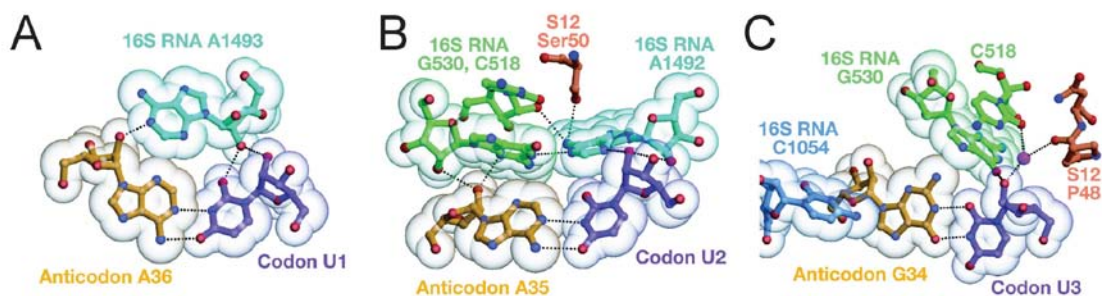


Figure 5. How the ribosome increases the intrinsic selectivity, d , of codon recognition. (A) The geometry of base pairing between U1 in first codon position and A36 in the anticodon is monitored by A1493. (B) The geometry of base pairing between U2 in second codon position and A35 in aminoacyl-tRNA is monitored by A1492 and G530, while the geometry of the base pairing in third codon position (U3:G34) is less stringently monitored, explaining the wobble hypothesis (From (Ogle and Ramakrishnan, 2005)).

In a next report from the Ramakrishnan laboratory, a small anticodon stem loop (ASL) analogue of tRNA^{Phe} was present in the A site of the crystal structure of the 30S subunit, along with a short mRNA sequence (U₆) cognate (UUU-codon in A site) to the ASL (Ogle et al., 2001). As predicted (Carter et al., 2000; Fourmy et al., 1998; Yoshizawa et al., 1999), binding of the ASL to the A site induced flipping out of the universally conserved bases A1492 and A1493 from the internal loop of helix 44 of 16S rRNA and caused a *syn* to *anti* conformational switch of the universally conserved base G530, allowing it to monitor the geometry of base pairing in the second position of the codon (Figure 5). It was also observed that binding of the cognate ASL to the 30S subunit changed it from an open to a more closed conformation (Figure 6). From the high resolution data, it was concluded that A1493 monitors the geometry of the first base pair of the codon-anticodon helix, A1492 and G530 monitor the second base pair, while the third base pair is less stringently monitored (Figure 5). These observations explained how the ribosome can monitor the geometry of the first two bases of the codon-anticodon helix by tRNA induced

movements of the three universally conserved bases 1492, 1493 and G530 in 16S rRNA. They could also for the first time offer an explanation for why the third base pair is much less stringently recognized on the ribosome, *i.e.* they provided a structural explanation for the wobble hypothesis (Figure 5).

In a third report on the accuracy of codon recognition, Ramakrishnan and collaborators (Ogle et al., 2002) studied the U₆ programmed 30S structure in complex with a cognate, ASL^{Phe}, as well as the near-cognate ASL^{Leu2} and ASL^{Ser} anticodon stem loops in the absence and presence of the error inducing drug paromomycin. They also performed biochemical experiments to determine the binding affinity of the cognate and near cognate ASLs in the presence and absence of paromomycin. Among the findings was that binding of the cognate ASL to the 30S subunit not only changed the positions of bases A1492, A1493 and G530 of 16S rRNA, but also induced a large conformational change of the subunit around the A site from an open to a closed form (Figure 6).

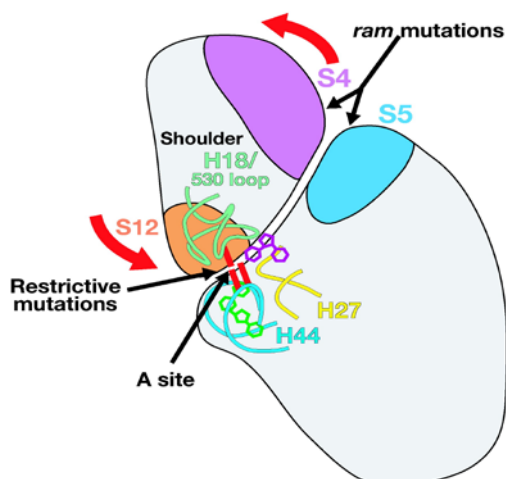


Figure 6. Closing and opening of the 30S subunit. The subunit opens and closes by intra-subunit rotations (red arrows) around the A site. The open conformation is stabilized by ribosomal proteins S4 and S5, while the closed conformation is stabilized by ribosomal protein S12. Cognate aminoacyl-tRNAs and some error inducing drugs (e.g. paromomycin) stabilize the closed conformation. Mutations in S12 tend to stabilize the open conformation (increased accuracy) and mutations in S4 and S5 tend to stabilize the closed conformation (decreased accuracy) (From (Ogle and Ramakrishnan, 2005)).

The near cognate ASLs were not seen in the A site without paromomycin, but could be observed in the presence of the drug with concomitant changes in the positions of the A1492, A1493 and G530 bases. Furthermore, the closed form of the 30S subunit was not induced in the presence of a near cognate ASL alone, and only appeared in the additional presence of paromomycin. From these data they inferred a model for tRNA recognition by the elongating ribosome, which can be briefly described as follows (Figures 2 and 6).

When a ternary complex cognate to the A-site codon binds to the ribosome, this induces movement of the bases A1492, A1493 and G530 of 16S rRNA so that they can interact with the minor groove of the first two positions of the codon-anticodon helix. This, in turn, drives the

30S subunit from its open towards its closed form (Figure 6), leading to rapid triggering of GTP hydrolysis on EF-Tu, release of EF-Tu in the GDP form, proofreading, accommodation of tRNA in A site and peptidyl-transfer (Figure 2).

When, in contrast, a non-cognate ternary complex binds to the A site in the absence of paromomycin or other error inducing drugs, bases A1492, A1493 and G530 do not bind to the codon-anticodon helix, there is no conformational change of the 30S subunit and thus no rapid triggering of GTP hydrolysis on EF-Tu. As a result, the near cognate ternary complex rapidly dissociates from the ribosome. This means that initial selection of ternary complex relies, firstly, on larger dissociation rates for a near-cognate, k_d^{nc} , than for cognate, k_d^c , ternary complex and, secondly, on faster GTP hydrolysis on EF-Tu for cognate (rate constant k_{GTP}^c) than non-cognate (rate constant k_{GTP}^{nc}) ternary complex. In the dissociation reactions, the geometrical monitoring of the codon-anticodon helix is absent so that the selectivity, $d_1 = k_d^{nc} / k_d^c$, is based on Watson-Crick base pairing. At the onset of the geometrical monitoring by the action of bases A1492, A1493 and G530, inducing the conformational change of the 30S subunit, the initial selectivity increases by a factor $d_2 = k_{GTP}^c / k_{GTP}^{nc}$ due to geometry monitoring, in line with kinetic experiments (Pape et al., 1999; 2001). The overall intrinsic accuracy of initial selection is therefore (See Figure 2)

$$d = d_1 \cdot d_2 = (k_d^{nc} / k_d^c) \cdot (k_{GTP}^c / k_{GTP}^{nc}) = e^{\Delta\Delta G^0 / RT}$$

Since the drug paromomycin stabilizes the closed conformation of the 30S subunit even in the presence of non-cognate aminoacyl-tRNAs, its presence brings the rate of GTP hydrolysis closer to the cognate rate. This reduces the ratio d_2 and thus the accuracy of cognate ternary complex selection.

There exist a large number of ribosomal ambiguity mutations (*ram*) which reduce the accuracy of tRNA selection. Many of these are caused by amino acid substitutions or deletions in ribosomal proteins S4 and S5. The 30S crystal structure shows that S4 and S5 stabilize the open 30S conformation (Figure 5), and their alteration by mutations is therefore likely to decrease the stability of the open in relation to the closed conformation. The RAM phenotype is explained as a stabilization of the closed in relation to the open 30S structure which facilitates the entry of near cognate tRNAs to the ribosome at unchanged rate of entry of cognate tRNAs. Ribosomal protein S12, in contrast, stabilizes the closed in relation to the open conformation, so that mutations in S12 are likely to favor the open form of the subunit. This leads to greatly reduced rate of A-site entry of near-cognate tRNAs at insignificantly reduced rate for cognate tRNAs, which explains the hyper-accurate phenotype associated with S12 mutations.

In summary, using a range of 30S structures at high resolution Ramakrishnan and collaborators have provided a simple and coherent explanation for a number of essential but hitherto poorly understood phenomena related to the accuracy of codon reading during mRNA translation.

Peptide bond formation and the 50S subunit structure

As soon as the 50S subunit structure from *H. marismortui* had been obtained at high resolution (Ban et al., 2000), it was anticipated that the mechanistic principles of how the ribosome catalyzes peptide bond formation by transferring the nascent peptide from the P-site peptidyl-tRNA to the A-site aminoacyl-tRNA would soon be understood (Figures 2 and 7). However, progress lingered and several hypotheses were proposed until a set of 50S structures from Steitz's group in conjunction with biochemical experiments and molecular computation efforts from other groups finally solved the riddle. One reason for the difficulty in obtaining a mechanistic understanding of the peptidyl-transfer mechanism can be traced to the difference between crystallographic characterization of a binding equilibrium on one hand and a catalytic mechanism on the other. In the latter case, one needs to understand not only the ground state with the reaction substrates but also the transition state. For this, the ribosome in complex with non-reactive substrate analogues, putative transition state and product analogues must be solved at high resolution. If the mechanism cannot be safely identified as analogous to a known mechanism, the crystal structure may have to be complemented with structurally based molecular computations that can tell whether a previously unknown mechanism can greatly reduce the transition state barrier in relation to a spontaneous reaction going through the same transition state.

The first decisive steps towards understanding peptide bond formation were provided by the two structures of the 50S subunit (Ban et al., 2000; Nissen et al., 2000). In the latter, the structure of the 50S subunit was solved with a putative puromycin derived transition state analogue (CCdAp-puromycin) and a stable N-aminoacylated minihelix functioning as an aminoacyl-tRNA analogue. Here, the three-dimensional structure of the peptidyl-transfer center of the 23S rRNA was outlined at high resolution for the very first time in the presence of a substrate or transition state analogue. Subsequently, Steitz, Moore and collaborators (Hansen et al., 2002) reported on new 50S subunit structures with novel analogues and further refinements of previous structures. In this work, they emphasized that the peptidyl-transfer center must carefully juxtapose the two substrates in peptide bond formation, but the mechanistic principles of catalysis remained elusive. However, the crystal complexes reported by (Hansen et al., 2002; Nissen et al., 2000) clearly defined the structural "boundary conditions" for peptidyl-transfer; and since then any proposed mechanism had to be compatible with important features of these crystal structures.

In 2004, Wolfenden, Rodnina and collaborators made an important contribution to the understanding of the catalytic mechanism of peptide bond formation. They studied the temperature dependence of the rate of peptidyl-transfer from a peptidyl-tRNA in the P site to the aminoacyl-tRNA analogue puromycin in the A site as well as of the rate of un-catalyzed peptide bond formation (Sievers et al., 2004). From these data they concluded that the ribosome does not lower the activation enthalpy of peptide bond formation but, surprisingly, increases it. The ribosome greatly reduces the activation entropy, meaning that catalysis is entropy rather than enthalpy driven. They speculated that the reduced activation enthalpy could emerge from the ribosome juxtaposing the peptidyl-transfer substrates already in their ribosome bound ground state, so that further substrate ordering would not be necessary in the transition state.

They also suggested an alternative explanation, *i.e.* that the reduced activation entropy could be caused by highly ordered water molecules.

Later in the same year, Strobel, Green and collaborators (Weinger et al., 2004) demonstrated quantitatively the essential nature of the 2'OH group of A76 of peptidyl-tRNA, with the peptidyl-moiety attached to O3' of A76 (Figure 7). For this, they used a dA76-substituted peptidyl-tRNA in the P site. They found that removal of the 2'-hydroxyl group reduced the rate of peptide bond formation by six orders of magnitude, and suggested *substrate* (*i.e.* the peptidyl-tRNA substrate in the P site) *catalyzed* peptide bond formation as essential for ribosomal peptidyl-transfer. This proposal was consistent with the positioning of A76 and its 2'-OH group within hydrogen bonding distance of the nucleophilic group of transition state analogues used by Steitz and collaborators (Hansen et al., 2002).

In 2005, molecular computation methods, based on previously published structures of the 50S subunits by Steitz, Moore and collaborators (Ban et al., 2000; Hansen et al., 2002; Nissen et al., 2000), were used to propose a mechanistic model for peptidyl-transfer (Trobroy and Åqvist, 2005). The authors predicted a network of hydrogen bonds, pre-organized in the ground state of the peptidyl-transfer reaction, and persisting through the transition state of peptide-bond formation (Trobroy and Åqvist, 2005, 2006). This pre-formed and persisting network of H-bonds explained why peptide bond formation on the ribosome is entropy, rather than enthalpy, driven, as earlier demonstrated experimentally (Sievers et al., 2004). According to the proposed mechanism, the 2'OH is part of a proton shuttling pathway (Dorner et al., 2003), removing the excess proton formed in the attack of the the α -amino group of the A-site aminoacyl-tRNA on the ester bond of the P-site tRNA (Figure 7). The suggested mechanism implicated ribosomal RNA and, in particular, 2'OH of A2451, as well as several water molecules as responsible for the network of H-bonds that greatly reduces the activation free energy in relation to the ground state in ribosome catalyzed peptide bond formation.

In the same year, Steitz and collaborators provided a new series of complexes of the 50S subunit with, in particular, improved resolution ($\sim 2.5\text{\AA}$) of details in the peptidyl-transfer centre (Schmeing et al., 2005a; Schmeing et al., 2005b). This crystallographic *tour de force* validated the proton shuttling role of 2'OH of A76 in P-site bound peptidyl-tRNA along with the network of H-bonds involving 23S rRNA bases and water molecules.

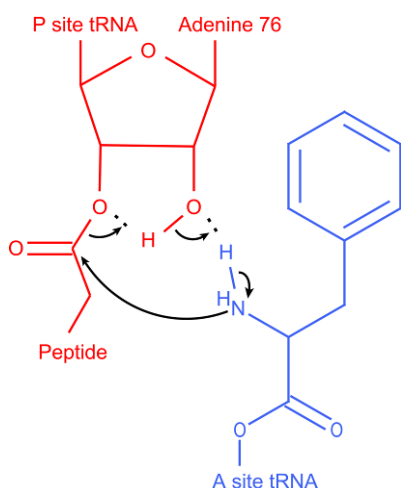


Figure 7. The mechanism of peptide bond formation on the ribosome.

The α -amino group of aminoacyl-tRNA in the A site (blue) attacks (black arrow right to left) the ester bond of the peptidyl-tRNA in the P site (red). A proton is shuttled via the OH' group of A76 in peptidyl-tRNA in the P site (black arrows left to right), aided by an H-bond network (Trobroy and Åqvist, 2005) established with the help of 23S rRNA bases and water molecules (not shown).

In summary, the 50S subunit structures from Steitz and collaborators, with the (Schmeing et al., 2005a) publication as the jewel in the crown, were instrumental in the clarification of how ribosomes catalyze peptide bonds. Biochemical work, often inspired by and interpreted in the light of these structures, was also important in this quest. Fundamental contributions were also made with molecular computation approaches, based on these very structures. For a review outlining additional aspects of how the mechanism of ribosomal peptide bond formation was clarified, see *e.g.* (Rodnina et al., 2007).

Ribosomal subunit structures and antibiotics

In the years after the Second World War, the wide spread introduction of antibiotics to treat bacterial infections revolutionized medicine and dramatically improved the health condition on a global scale. Now, 60 years later, the ever evolving antibiotic resistance among pathogens has heavily depleted the arsenal of effective antibiotic drugs. We seem to be running out of options, and a return to the pitiful health conditions preceding the Second World War has become an ominous scenario. About 90 000 patients in the USA die yearly as a result of bacterial infections compared to only about 13 000 twenty years ago, and in the majority of these casualties antibiotic resistance is an aggravating factor.

In recent years structure-based drug design (SBDD), where high resolution structures of drug targets and their resistance mutants are used to create novel drugs, has scored some promising successes, *e.g.* in the quest against HIV-virus infections. The ribosome is the target for about 50% of all antibacterial drugs to date, and the advent of high resolution structures of both ribosomal subunits has opened a large number of possibilities for SBDD of new and effective drugs in the race against resistance development among bacterial pathogens. For instance, many different types of antibiotic drugs bind to the peptidyl-transfer center of the 50S subunit of the bacterial ribosome (Fig. 8).

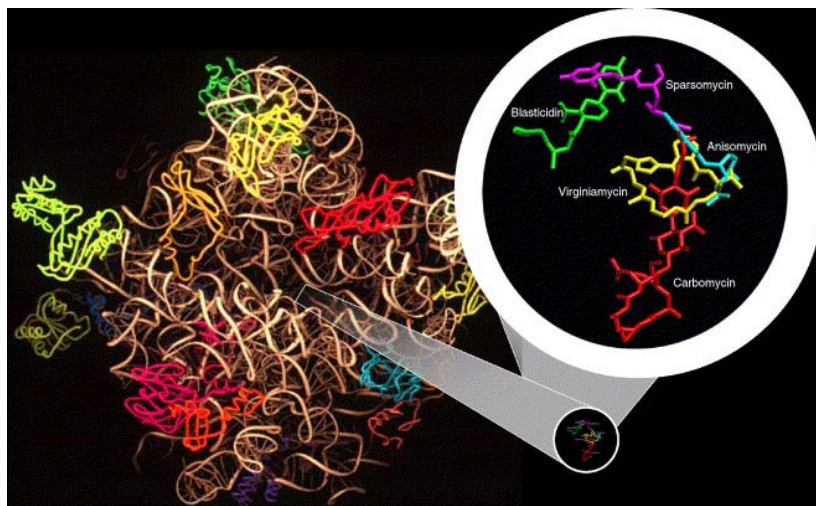


Figure 8. The peptidyl-transferase center in the 50S ribosomal subunit is attacked by a large number of existing antibiotics, now revealed at high resolution in 50S subunit crystal structures (Figure 8) (Franceschi and Duffy, 2006).

The binding modes of a large number of antibiotic drugs to the 30S (Figure 9a) and 50S (Figure 9b) subunit have now been revealed at high resolution, and serve as leads for the design of novel drugs.

Table 1a – Available structures of antibiotics targeting the small ribosomal subunit (30S)

Proposed mechanism of action	Antibiotic class	Antibiotic	Refs.	PDB ID	System used for structural determination
Bind to A- or P-sites and affect decoding.	Aminoglycosides	Apramycin	[66]	1YRJ	RNA fragment
		Geneticin	[67]	1MWL	RNA fragment
		Hygromycin B	[68]	1HNZ	<i>T. thermophilus</i>
		Paromomycin	[26]	1FJG	<i>T. thermophilus</i>
		Paromomycin	[48]	1IBK	<i>T. thermophilus</i>
		Paromomycin	[25]	1J7T	RNA fragment
		Tobramycin	[50]	1LC4	RNA fragment
		Streptomycin	[26]	1FJG	<i>T. thermophilus</i>
Block binding of A-site tRNA	Tetracyclines	Tetracycline	[68]	1HNW	<i>T. thermophilus</i>
		Tetracycline	[69]	1I97	<i>T. thermophilus</i>
Inhibit translocation	Various	Edeine	[69]	1I95	<i>T. thermophilus</i>
		Pactamycin	[68]	1HNX	<i>T. thermophilus</i>
		Spectinomycin	[26]	1FJG	<i>T. thermophilus</i>

Figure 9a. Tabulation of 30S crystal structures in complex with antibiotic drugs. A survey of *T. Thermophilus* 30S subunit structures at high resolution containing various antibiotic drugs in existence by year 2006 is shown in Figure 9a, i.e. table 1a of (Franceschi and Duffy, 2006). Numbers [26, 48, 68] in the table refer to Ramakrishnan's 30S subunit structures (Brodersen et al., 2000; Carter et al., 2000; Ogle et al., 2001), while number [69] refers to Yonath's 30S structure from the same organism (Pioletti et al., 2001).

Table 1b – Available structures of antibiotics targeting the large ribosomal subunit (50S)

Proposed mechanism of action	Antibiotic class	Antibiotic	Refs.	PDB ID	System used for structural determination
Block peptide bond formation by interfering with A-site or P-site tRNA and/or prevent the elongation of the nascent peptide	Macrolides	Azithromycin	[70]	1M1K	<i>H. marismortui</i>
		Azithromycin	[71]	1NWX	<i>D. radiodurans</i>
		Azithromycin	[19]	1YHQ	<i>H. marismortui</i> (G2058A)
		Erythromycin	[72]	1JZY	<i>D. radiodurans</i>
		Carbomycin	[70]	1K8A	<i>H. marismortui</i>
		Erythromycin	[19,79]	1YI2	<i>H. marismortui</i> (G2058A)
		Clarithromycin	[72]	1J5A	<i>D. radiodurans</i>
		Roxithromycin	[72]	1JZZ	<i>D. radiodurans</i>
		Spiramycin	[70]	1KD1	<i>H. marismortui</i>
		Troleandomycin	[73]	1OND	<i>D. radiodurans</i>
	Tylosin	[70]	1K9M	<i>H. marismortui</i>	
	Ketolides	ABT-773	[71]	1NWX	<i>D. radiodurans</i>
		Telithromycin	[74,79]	1P9X	<i>D. radiodurans</i>
		Telithromycin	[19]	1YIJ	<i>H. marismortui</i> (G2058A)
		Streptogramins	Dalfopristin	[75]	1SM1
	Quinupristin		[75]	1SM1	<i>D. radiodurans</i>
	Quinupristin		[19]	1YJW	<i>H. marismortui</i> (G2058A)
	Virginiamycin S		[19]	1YIT	<i>H. marismortui</i> (G2058A)
	Virginiamycin M		[76]	1N8R	<i>H. marismortui</i>
	Lincosamides	Virginiamycin M	[19]	1YIT	<i>H. marismortui</i> (G2058A)
		Clindamycin	[72,79]	1JZX	<i>D. radiodurans</i>
		Clindamycin	[19]	1YJN	<i>H. marismortui</i> (G2058A)
	Pleuromutilins	Tiamulin	[77]	1XBP	<i>D. radiodurans</i>
		Phenyl propanoids	Chloramphenicol	[72]	1K01
	Chloramphenicol		[76]	1NJ1	<i>H. marismortui</i>
	Oxazolidinones	Linezolid	[61]	Not available	<i>H. marismortui</i>
		Various	Puromycin	[78]	1FFZ
Sparsomycin	[76]		1M90	<i>H. marismortui</i>	
Anisomycin	[76]		1K73	<i>H. marismortui</i>	
Blasticidin S	[76]		1KCS	<i>H. marismortui</i>	

The PDB ID refers to the Protein Data Bank (PDB) identification code of each structure. The atomic coordinates for each structure can be downloaded from <http://www.pdb.org> using their respective PDB IDs.

Figure 9b. Tabulation of 50S crystal structures in complex with antibiotic drugs. A survey of 50S subunit structures at high resolution containing various antibiotic drugs by the year 2006 is shown in Figure 9b, i.e. table 1b of (Franceschi and Duffy, 2006). In general the *H. marismortui* 50S subunit structures originate from Steitz's and the *D. radiodurans* 50S subunit structures from Yonath's laboratory.

Turning another page: a new generation of functional crystal complexes of the ribosome

Termination of protein synthesis: reading of mRNA stop codons by proteins.

Termination of protein synthesis by hydrolysis of the ester bond, linking a finished protein to the tRNA in P site, induced by the stop codon reading proteins RF1 and RF2 (see Section 1 above) has posed a number fundamental questions, which have remained unanswered over decades. Among these are (i) How can RF1 and RF2 efficiently recognize the three stop (non-sense) codons and, at the same time, in the absence of proofreading precisely discriminate against premature termination at any of the 61 sense codons? (Freistroffer et al., 2000) (ii) How do RF1 and RF2 induce ester bond hydrolysis in the P-site peptidyl-tRNA during termination and, in particular (iii) What role is played by the universally conserved GGQ motif in class-1 release factors (Frolova et al., 1999)? Neither low-resolution cryo-EM (Klaholz et al., 2003; Rawat et al., 2006; Rawat et al., 2003) nor mid-resolution crystallography (Petry et al., 2005) could answer these questions. The situation changed dramatically with a report from Noller's group of a high resolution (3.1Å) structure of the *T. thermophilus* ribosome in termination complex with RF1 (Laurberg et al., 2008). Soon after, the Ramakrishnan (Weixlbaumer et al., 2008) and Noller (Korostelev et al., 2008) groups reported high resolution structures of the *T. thermophilus* ribosome in termination complex with RF2. These structures have led to a revision of previous suggestions that the RFs have anticodon-like peptide loops in analogy with tRNA anticodons that read the stop codons (Nakamura and Ito, 1998). They also provide the keys to quantitative, atomic level understanding of all aspects of stop codon reading and the involvement of the universally conserved GGQ-loop in inducing ester bond hydrolysis in the last peptidyl-tRNA during the synthesis of a protein.

The enigmatic LepA and EF-P proteins. LepA is a GTPase with strongly conserved peptide sequence among bacteria, in mitochondria and chloroplasts. It was recently discovered, that LepA catalyzes reverse translocation of tRNAs and mRNA and it has been speculated that LepA corrects translocation as well as other types of errors during protein elongation (Qin et al., 2006). A high resolution (2.8Å) structure of LepA has now been reported from the Steitz laboratory, clarifying aspects of the factor's reverse translocation activity (Connell et al., 2008).

Elongation factor EF-P is a translation factor conserved among bacteria with eIF-5A as its eukaryote homologue. The high resolution structure of the ribosome in complex with EF-P reported by Steitz and collaborators (Blaha et al., 2009) reveals the binding site of the protein to be between the E and P sites of the ribosome. The structure suggests how EF-P could facilitate the proper positioning of the fMet-tRNA^{fMet} for rapid formation of the first peptide bond after translation initiation.

High resolution crystal structures of the ribosome in elongation phase. In 2006 Ramakrishnan and collaborators reported a high resolution (2.8Å) crystal structure of the 70S ribosome from *T. Thermophilus* in pre-translocation state (Selmer et al., 2006), illustrated at cryo-EM resolution in Figure 3B above. From this structure, models were constructed of the tRNA and mRNA structures in the ribosome and how they interact with the ribosome.

More recently, Ramakrishnan and collaborators reported high resolution crystal structures of two ribosomal complexes, also from *T. thermophilus* (Voorhees et al., 2009). These revealed that extended peptide sequences of ribosomal proteins L27 and L16 of the 50S subunit stabilize the CCA-ends of both tRNAs in the peptidyl-transfer reaction, suggesting that peptide chains from both these proteins take part in the catalytic mechanism of peptide bond formation, in line with previous biochemical data (Hampl et al., 1981; Kazemie, 1976; Maguire et al., 2005; Moore et al., 1975). The *archaeon* *H. marismortui* lacks these proteins, but Voorhees et al. speculated that a peptide chain in ribosomal protein L10e in the 50S subunit of *H. marismortui* may extend all the way into the peptidyl-transferase center and there play the same role as L27 in bacteria. The reason why the extended peptide chain was not seen in Steitz's 50S structures could, they proposed, be due to its mobility in the absence of stably bound native tRNAs in the A and P sites. If so, this could mean that although tRNA and rRNA are the principal catalysts of peptide bond formation, ribosomal proteins may also play a significant role in this reaction in *bacteria* and perhaps also in *archaea* and *eukarya*.

Colophon. In the beginning it was generally believed that ribosomal protein carried out the ribosome's catalytic actions. Then it was believed that ribosomal RNA was the catalyst. Now, we know that peptide bond formation on the bacterial ribosome and perhaps on the ribosomes from all organisms is catalyzed by ribosomal RNA as well as ribosomal protein and also by the 2'-OH group of the peptidyl-tRNA substrate in the P site (Figure 7). This catalytic triad of ribosomal RNA, ribosomal protein and tRNA substrate may reflect a more complex starting point for the route to the present protein dominated world than a pure RNA world.

Conclusions

Ramakrishnan, Steitz and Yonath have made ground breaking contributions to the crystallography of ribosomes and used high-resolution functional ribosome complexes to clarify long-standing and fundamental questions in protein synthesis. Their work has far-reaching implications for basic science and medicine.

Uppsala 30 September 2009

Måns Ehrenberg

References

- Antoun, A., Pavlov, M.Y., Lovmar, M., and Ehrenberg, M. (2006). How initiation factors tune the rate of initiation of protein synthesis in bacteria. *The EMBO journal* **25**, 2539-2550.
- Ban, N., Freeborn, B., Nissen, P., Penczek, P., Grassucci, R.A., Sweet, R., Frank, J., Moore, P.B., and Steitz, T.A. (1998). A 9 Å resolution X-ray crystallographic map of the large ribosomal subunit. *Cell* **93**, 1105-1115.
- Ban, N., Nissen, P., Hansen, J., Capel, M., Moore, P.B., and Steitz, T.A. (1999). Placement of protein and RNA structures into a 5 Å-resolution map of the 50S ribosomal subunit. *Nature* **400**, 841-847.
- Ban, N., Nissen, P., Hansen, J., Moore, P.B., and Steitz, T.A. (2000). The complete atomic structure of the large ribosomal subunit at 2.4 Å resolution. *Science* **289**, 905-920.
- Blaha, G., Stanley, R.E., and Steitz, T.A. (2009). Formation of the first peptide bond: the structure of EF-P bound to the 70S ribosome. *Science* **325**, 966-970.
- Brodersen, D.E., Clemons, W.M., Jr., Carter, A.P., Morgan-Warren, R.J., Wimberly, B.T., and Ramakrishnan, V. (2000). The structural basis for the action of the antibiotics tetracycline, pactamycin, and hygromycin B on the 30S ribosomal subunit. *Cell* **103**, 1143-1154.
- Carter, A.P., Clemons, W.M., Brodersen, D.E., Morgan-Warren, R.J., Wimberly, B.T., and Ramakrishnan, V. (2000). Functional insights from the structure of the 30S ribosomal subunit and its interactions with antibiotics. *Nature* **407**, 340-348.
- Cate, J.H., Yusupov, M.M., Yusupova, G.Z., Earnest, T.N., and Noller, H.F. (1999). X-ray crystal structures of 70S ribosome functional complexes. *Science* **285**, 2095-2104.
- Clemons, W.M., Jr., May, J.L., Wimberly, B.T., McCutcheon, J.P., Capel, M.S., and Ramakrishnan, V. (1999). Structure of a bacterial 30S ribosomal subunit at 5.5 Å resolution. *Nature* **400**, 833-840.
- Connell, S.R., Topf, M., Qin, Y., Wilson, D.N., Mielke, T., Fucini, P., Nierhaus, K.H., and Spahn, C.M. (2008). A new tRNA intermediate revealed on the ribosome during EF4-mediated back-translocation. *Nat Struct Mol Biol* **15**, 910-915.
- Crick, F. (1970). Central dogma of molecular biology. *Nature* **227**, 561-563.
- Crick, F.H. (1958). On protein synthesis. *Symposia of the Society for Experimental Biology* **12**, 138-163.
- Crick, F.H. (1966). Codon-anticodon pairing: the wobble hypothesis. *J Mol Biol* **19**, 548-555.
- Dorner, S., Panuschka, C., Schmid, W., and Barta, A. (2003). Mononucleotide derivatives as ribosomal P-site substrates reveal an important contribution of the 2'-OH to activity. *Nucleic acids research* **31**, 6536-6542.
- Ehrenberg, M., and Blomberg, C. (1980). Thermodynamic constraints on kinetic proofreading in biosynthetic pathways. *Biophys J* **31**, 333-358.
- Fourmy, D., Recht, M.I., and Puglisi, J.D. (1998). Binding of neomycin-class aminoglycoside antibiotics to the A-site of 16 S rRNA. *J Mol Biol* **277**, 347-362.

Franceschi, F., and Duffy, E.M. (2006). Structure-based drug design meets the ribosome. *Biochemical pharmacology* *71*, 1016-1025.

Frank, J., Gao, H., Sengupta, J., Gao, N., and Taylor, D.J. (2007). The process of mRNA-tRNA translocation. *Proc Natl Acad Sci U S A* *104*, 19671-19678.

Frank, J., Zhu, J., Penczek, P., Li, Y., Srivastava, S., Verschoor, A., Radermacher, M., Grassucci, R., Lata, R.K., and Agrawal, R.K. (1995). A model of protein synthesis based on cryo-electron microscopy of the *E. coli* ribosome. *Nature* *376*, 441-444.

Freistroffer, D.V., Kwiatkowski, M., Buckingham, R.H., and Ehrenberg, M. (2000). The accuracy of codon recognition by polypeptide release factors. *Proc Natl Acad Sci U S A* *97*, 2046-2051.

Freter, R.R., and Savageau, M.A. (1980). Proofreading systems of multiple stages for improved accuracy of biological discrimination. *J Theor Biol* *85*, 99-123.

Frolova, L.Y., Tsivkovskii, R.Y., Sivolobova, G.F., Oparina, N.Y., Serpinsky, O.I., Blinov, V.M., Tatkov, S.I., and Kisselev, L.L. (1999). Mutations in the highly conserved GGQ motif of class 1 polypeptide release factors abolish ability of human eRF1 to trigger peptidyl-tRNA hydrolysis. *Rna* *5*, 1014-1020.

Garman, E. (1999). Cool data: quantity AND quality. *Acta crystallographica* *55*, 1641-1653.

Glutz, C., Mussig, J., Gewitz, H.S., Makowski, I., Arad, T., Yonath, A., and Wittmann, H.G. (1987). Three-dimensional crystals of ribosomes and their subunits from eu- and archaebacteria. *Biochem Int* *15*, 953-960.

Gromadski, K.B., and Rodnina, M.V. (2004). Kinetic determinants of high-fidelity tRNA discrimination on the ribosome. *Mol Cell* *13*, 191-200.

Hampl, H., Schulze, H., and Nierhaus, K.H. (1981). Ribosomal components from *Escherichia coli* 50 S subunits involved in the reconstitution of peptidyltransferase activity. *J Biol Chem* *256*, 2284-2288.

Hansen, J.L., Schmeing, T.M., Moore, P.B., and Steitz, T.A. (2002). Structural insights into peptide bond formation. *Proc Natl Acad Sci U S A* *99*, 11670-11675.

Harms, J., Schluenzen, F., Zarivach, R., Bashan, A., Gat, S., Agmon, I., Bartels, H., Franceschi, F., and Yonath, A. (2001). High resolution structure of the large ribosomal subunit from a mesophilic eubacterium. *Cell* *107*, 679-688.

Hendrickson, W.A., Ogata, C.M., and Charles W. Carter, Jr. (1997). [28] Phase determination from multiwavelength anomalous diffraction measurements. In *Methods in enzymology* (Academic Press), pp. 494-523.

Holmes, K.C., and Rosenbaum, G. (1998). How X-ray Diffraction with Synchrotron Radiation Got Started. *Journal of synchrotron radiation* *5*, 147-153.

Hope, H., Frolow, F., von Bohlen, K., Makowski, I., Kratky, C., Halfon, Y., Danz, H., Webster, P., Bartels, K.S., Wittmann, H.G., and et al. (1989). Cryocrystallography of ribosomal particles. *Acta crystallographica* *45 (Pt 2)*, 190-199.

Karimi, R., Pavlov, M.Y., Buckingham, R.H., and Ehrenberg, M. (1999). Novel roles for classical factors at the interface between translation termination and initiation. *Molecular cell* *3*, 601-609.

- Kazemie, M. (1976). Binding of aminoacyl-tRNA to reconstituted subparticles of *Escherichia coli* large ribosomal subunits. *Eur J Biochem* *67*, 373-378.
- Kisselev, L.L., and Buckingham, R.H. (2000). Translational termination comes of age. *Trends in biochemical sciences* *25*, 561-566.
- Klaholz, B.P., Pape, T., Zavialov, A.V., Myasnikov, A.G., Orlova, E.V., Vestergaard, B., Ehrenberg, M., and van Heel, M. (2003). Structure of the *Escherichia coli* ribosomal termination complex with release factor 2. *Nature* *421*, 90-94.
- Kornberg, A. (1969). Active center of DNA polymerase. *Science* *163*, 1410-1418.
- Kornberg, R.D. (2007). The molecular basis of eukaryotic transcription. *Proc Natl Acad Sci U S A* *104*, 12955-12961.
- Korostelev, A., Asahara, H., Lancaster, L., Laurberg, M., Hirschi, A., Zhu, J., Trakhanov, S., Scott, W.G., and Noller, H.F. (2008). Crystal structure of a translation termination complex formed with release factor RF2. *Proc Natl Acad Sci U S A* *105*, 19684-19689.
- Laurberg, M., Asahara, H., Korostelev, A., Zhu, J., Trakhanov, S., and Noller, H.F. (2008). Structural basis for translation termination on the 70S ribosome. *Nature* *454*, 852-857.
- Maguire, B.A., Beniaminov, A.D., Ramu, H., Mankin, A.S., and Zimmermann, R.A. (2005). A protein component at the heart of an RNA machine: the importance of protein l27 for the function of the bacterial ribosome. *Mol Cell* *20*, 427-435.
- Makowski, I., Frolow, F., Saper, M.A., Shoham, M., Wittmann, H.G., and Yonath, A. (1987). Single crystals of large ribosomal particles from *Halobacterium marismortui* diffract to 6 Å. *J Mol Biol* *193*, 819-822.
- Moore, V.G., Atchison, R.E., Thomas, G., Moran, M., and Noller, H.F. (1975). Identification of a ribosomal protein essential for peptidyl transferase activity. *Proceedings of the National Academy of Sciences of the United States of America* *72*, 844-848.
- Nakamura, Y., and Ito, K. (1998). How protein reads the stop codon and terminates translation. *Genes Cells* *3*, 265-278.
- Nirenberg, M., Leder, P., Bernfield, M., Brimacombe, R., Trupin, J., Rottman, F., and O'Neal, C. (1965). RNA codewords and protein synthesis, VII. On the general nature of the RNA code. *Proc Natl Acad Sci U S A* *53*, 1161-1168.
- Nissen, P., Hansen, J., Ban, N., Moore, P.B., and Steitz, T.A. (2000). The structural basis of ribosome activity in peptide bond synthesis. *Science* *289*, 920-930.
- Noller, H.F., Hoffarth, V., and Zimniak, L. (1992). Unusual resistance of peptidyl transferase to protein extraction procedures. *Science* *256*, 1416-1419.
- Ogle, J.M., Brodersen, D.E., Clemons, W.M., Jr., Tarry, M.J., Carter, A.P., and Ramakrishnan, V. (2001). Recognition of cognate transfer RNA by the 30S ribosomal subunit. *Science* *292*, 897-902.
- Ogle, J.M., Murphy, F.V., Tarry, M.J., and Ramakrishnan, V. (2002). Selection of tRNA by the ribosome requires a transition from an open to a closed form. *Cell* *111*, 721-732.
- Ogle, J.M., and Ramakrishnan, V. (2005). Structural insights into translational fidelity. *Annu Rev Biochem* *74*, 129-177.

Pape, T., Wintermeyer, W., and Rodnina, M. (1999). Induced fit in initial selection and proofreading of aminoacyl-tRNA on the ribosome. *Embo J* 18, 3800-3807.

Petry, S., Brodersen, D.E., Murphy, F.V.t., Dunham, C.M., Selmer, M., Tarry, M.J., Kelley, A.C., and Ramakrishnan, V. (2005). Crystal structures of the ribosome in complex with release factors RF1 and RF2 bound to a cognate stop codon. *Cell* 123, 1255-1266.

Phillips, J.C., Wlodawer, A., Goodfellow, J.M., Watenpaugh, K.D., Sieker, L.C., Jensen, L.H., and Hodgson, K.O. (1977). Applications of synchrotron radiation to protein crystallography. II. Anomalous scattering, absolute intensity and polarization. *Acta Crystallogr* A33, 445-455.

Pioletti, M., Schlunzen, F., Harms, J., Zarivach, R., Gluhmann, M., Avila, H., Bashan, A., Bartels, H., Auerbach, T., Jacobi, C., *et al.* (2001). Crystal structures of complexes of the small ribosomal subunit with tetracycline, edeine and IF3. *Embo J* 20, 1829-1839.

Qin, Y., Polacek, N., Vesper, O., Staub, E., Einfeldt, E., Wilson, D.N., and Nierhaus, K.H. (2006). The highly conserved LepA is a ribosomal elongation factor that back-translocates the ribosome. *Cell* 127, 721-733.

Rawat, U., Gao, H., Zavialov, A., Gursky, R., Ehrenberg, M., and Frank, J. (2006). Interactions of the release factor RF1 with the ribosome as revealed by cryo-EM. *J Mol Biol* 357, 1144-1153.

Rawat, U.B., Zavialov, A.V., Sengupta, J., Valle, M., Grassucci, R.A., Linde, J., Vestergaard, B., Ehrenberg, M., and Frank, J. (2003). A cryo-electron microscopic study of ribosome-bound termination factor RF2. *Nature* 421, 87-90.

Rodnina, M.V., Beringer, M., and Wintermeyer, W. (2007). How ribosomes make peptide bonds. *Trends in biochemical sciences* 32, 20-26.

Ruusala, T., Ehrenberg, M., and Kurland, C.G. (1982). Is there proofreading during polypeptide synthesis? *Embo J* 1, 741-745.

Schlunzen, F., Tocilj, A., Zarivach, R., Harms, J., Gluehmann, M., Janell, D., Bashan, A., Bartels, H., Agmon, I., Franceschi, F., and Yonath, A. (2000). Structure of functionally activated small ribosomal subunit at 3.3 angstroms resolution. *Cell* 102, 615-623.

Schmeing, T.M., Huang, K.S., Kitchen, D.E., Strobel, S.A., and Steitz, T.A. (2005a). Structural insights into the roles of water and the 2' hydroxyl of the P site tRNA in the peptidyl transferase reaction. *Mol Cell* 20, 437-448.

Schmeing, T.M., Huang, K.S., Strobel, S.A., and Steitz, T.A. (2005b). An induced-fit mechanism to promote peptide bond formation and exclude hydrolysis of peptidyl-tRNA. *Nature* 438, 520-524.

Schuwirth, B.S., Borovinskaya, M.A., Hau, C.W., Zhang, W., Vila-Sanjurjo, A., Holton, J.M., and Cate, J.H. (2005). Structures of the bacterial ribosome at 3.5 Å resolution. *Science* 310, 827-834.

Selmer, M., Dunham, C.M., Murphy, F.V.t., Weixlbaumer, A., Petry, S., Kelley, A.C., Weir, J.R., and Ramakrishnan, V. (2006). Structure of the 70S ribosome complexed with mRNA and tRNA. *Science* 313, 1935-1942.

Shevack, A., Gewitz, H.S., Hennemann, B., Yonath, A., and Wittmann, H.G. (1985). Characterization and crystallization of ribosomal particles from *Halobacterium marismortui*. *FEBS Lett* 184, 68-71.

Sievers, A., Beringer, M., Rodnina, M.V., and Wolfenden, R. (2004). The ribosome as an entropy trap. *Proc Natl Acad Sci U S A* *101*, 7897-7901.

Soll, D., Ohtsuka, E., Jones, D.S., Lohrmann, R., Hayatsu, H., Nishimura, S., and Khorana, H.G. (1965). Studies on polynucleotides, XLIX. Stimulation of the binding of aminoacyl-sRNA's to ribosomes by ribotrinnucleotides and a survey of codon assignments for 20 amino acids. *Proc Natl Acad Sci U S A* *54*, 1378-1385.

Thompson, R.C., and Stone, P.J. (1977). Proofreading of the codon-anticodon interaction on ribosomes. *Proceedings of the National Academy of Sciences of the United States of America* *74*, 198-202.

Tocilj, A., Schlunzen, F., Janell, D., Gluhmann, M., Hansen, H.A., Harms, J., Bashan, A., Bartels, H., Agmon, I., Franceschi, F., and Yonath, A. (1999). The small ribosomal subunit from *Thermus thermophilus* at 4.5 Å resolution: pattern fittings and the identification of a functional site. *Proc Natl Acad Sci U S A* *96*, 14252-14257.

Trakhanov, S.D., Yusupov, M.M., Agalarov, S.C., Garber, M.B., Ryazantsev, S.N., Tischenko, S.V., and Shirokov, V.A. (1987). Crystallization of 70 S ribosomes and 30 S ribosomal subunits from *Thermus thermophilus*. *FEBS Lett* *220*, 319-322.

Trobro, S., and Åqvist, J. (2005). Mechanism of peptide bond synthesis on the ribosome. *Proc Natl Acad Sci U S A* *102*, 12395-12400.

Trobro, S., and Åqvist, J. (2006). Analysis of predictions for the catalytic mechanism of ribosomal peptidyl transfer. *Biochemistry* *45*, 7049-7056.

Valle, M., Zavialov, A., Li, W., Stagg, S.M., Sengupta, J., Nielsen, R.C., Nissen, P., Harvey, S.C., Ehrenberg, M., and Frank, J. (2003). Incorporation of aminoacyl-tRNA into the ribosome as seen by cryo-electron microscopy. *Nature structural biology* *10*, 899-906.

von Bohlen, K., Makowski, I., Hansen, H.A., Bartels, H., Berkovitch-Yellin, Z., Zaytzev-Bashan, A., Meyer, S., Paulke, C., Franceschi, F., and Yonath, A. (1991). Characterization and preliminary attempts for derivatization of crystals of large ribosomal subunits from *Haloarcula marismortui* diffracting to 3 Å resolution. *J Mol Biol* *222*, 11-15.

Voorhees, R.M., Weixlbaumer, A., Loakes, D., Kelley, A.C., and Ramakrishnan, V. (2009). Insights into substrate stabilization from snapshots of the peptidyl transferase center of the intact 70S ribosome. *Nat Struct Mol Biol* *16*, 528-533.

Watson, J.D., and Crick, F.H. (1953a). Genetical implications of the structure of deoxyribonucleic acid. *Nature* *171*, 964-967.

Watson, J.D., and Crick, F.H. (1953b). Molecular structure of nucleic acids; a structure for deoxyribose nucleic acid. *Nature* *171*, 737-738.

Weinger, J.S., Parnell, K.M., Dorner, S., Green, R., and Strobel, S.A. (2004). Substrate-assisted catalysis of peptide bond formation by the ribosome. *Nat Struct Mol Biol* *11*, 1101-1106.

Weixlbaumer, A., Jin, H., Neubauer, C., Voorhees, R.M., Petry, S., Kelley, A.C., and Ramakrishnan, V. (2008). Insights into translational termination from the structure of RF2 bound to the ribosome. *Science* *322*, 953-956.

Wimberly, B.T., Brodersen, D.E., Clemons, W.M., Jr., Morgan-Warren, R.J., Carter, A.P., Vornhein, C., Hartsch, T., and Ramakrishnan, V. (2000). Structure of the 30S ribosomal subunit. *Nature* *407*, 327-339.

Yonath, A., Bartunik, H.D., Bartels, K.S., and Wittmann, H.G. (1984). Some x-ray diffraction patterns from single crystals of the large ribosomal subunit from *Bacillus stearothermophilus*. *J Mol Biol* *177*, 201-206.

Yonath, A., Mussig, J., Tesche, B., Lorenz, S., Erdmann, V.A., and Wittmann, H.G. (1980). Crystallization of the large ribosomal subunits from *Bacillus stearothermophilus*. *Biochem Int* *1*, 428-435.

Yoshizawa, S., Fourmy, D., and Puglisi, J.D. (1999). Recognition of the codon-anticodon helix by ribosomal RNA. *Science (New York, N.Y)* *285*, 1722-1725.

Yusupov, M.M., Yusupova, G.Z., Baucom, A., Lieberman, K., Earnest, T.N., Cate, J.H., and Noller, H.F. (2001). Crystal structure of the ribosome at 5.5 Å resolution. *Science* *292*, 883-896.

Zavialov, A.V., Mora, L., Buckingham, R.H., and Ehrenberg, M. (2002). Release of peptide promoted by the GGQ motif of class 1 release factors regulates the GTPase activity of RF3. *Mol Cell* *10*, 789-798.